





Article

Design, Synthesis, and Antisickling Investigation of a Nitric Oxide-Releasing Prodrug of 5HMF for the Treatment of Sickle Cell Disease

Rana T. Alhashimi ¹, Mohini S. Ghatge ¹, Akua K. Donkor ¹, Tanvi M. Deshpande ², Nancy Anabaraonye ³, Dina Alramadhani ¹, Richmond Danso-Danquah ¹, Boshi Huang ¹, Yan Zhang ¹, Faik N. Musayev ¹, Osheiza Abdulmalik ^{3,†} and Martin K. Safo ^{1,*,†}

¹ Department of Medicinal Chemistry and The Institute for Structural Biology, Drug Discovery and Development, School of Pharmacy, Virginia Commonwealth University, Richmond, VA 23298, USA; alhashimirt@vcu.edu (R.T.A.); msghatge@vcu.edu (M.S.G.); donkora@vcu.edu (A.K.D.); alramadhanid@vcu.edu (D.A.); rddanso@gmail.com (R.D.-D.); bhuang2@vcu.edu (B.H.); yzhang2@vcu.edu (Y.Z.); fmoussae@vcu.edu (F.N.M.)

² Vertex Pharmaceutical Incorporated, Boston, MA 02210, USA; deshbandetm@gmail.com

³ Division of Hematology, The Children's Hospital of Philadelphia, Philadelphia, PA 19104, USA; Nancyaa@sas.upenn.edu (N.A.); abdulmalik@email.chop.edu (O.A.)

* Correspondence: msaf@vcu.edu; Tel.: +1-(804)-828-7291

† Martin K. Safo and Osheiza Abdulmalik are co-senior authors.



Citation: Alhashimi, R.T.; Ghatge, M.S.; Donkor, A.K.; Deshpande, T.M.; Anabaraonye, N.; Alramadhani, D.; Danso-Danquah, R.; Huang, B.; Zhang, Y.; Musayev, F.N.; et al. Design, Synthesis, and Antisickling Investigation of a Nitric Oxide-Releasing Prodrug of 5HMF for the Treatment of Sickle Cell Disease. *Biomolecules* **2022**, *12*, 696. <https://doi.org/10.3390/biom12050696>

Academic Editor: Loredana Salerno

Received: 5 April 2022

Accepted: 10 May 2022

Published: 12 May 2022

Publisher's Note: MDPI stays neutral with regard to jurisdictional claims in published maps and institutional affiliations.



Copyright: © 2022 by the authors. Licensee MDPI, Basel, Switzerland. This article is an open access article distributed under the terms and conditions of the Creative Commons Attribution (CC BY) license (<https://creativecommons.org/licenses/by/4.0/>).

Abstract: 5-hydroxyfurfural (5HMF), an allosteric effector of hemoglobin (Hb) with an ability to increase Hb affinity for oxygen has been studied extensively for its antisickling effect in vitro and in vivo, and in humans for the treatment of sickle cell disease (SCD). One of the downstream pathophysiologicals of SCD is nitric oxide (NO) deficiency, therefore increasing NO (bio)availability is known to mitigate the severity of SCD symptoms. We report the synthesis of an NO-releasing prodrug of 5HMF (5HMF-NO), which in vivo, is expected to be bio-transformed into 5HMF and NO, with concomitant therapeutic activities. In vitro studies showed that when incubated with whole blood, 5HMF-NO releases NO, as anticipated. When incubated with sickle blood, 5HMF-NO formed Schiff base adduct with Hb, increased Hb affinity for oxygen, and prevented hypoxia-induced erythrocyte sickling, which at 1 mM concentration were 16%, 10% and 27%, respectively, compared to 21%, 18% and 21% for 5HMF. Crystal structures of 5HMF-NO with Hb showed 5HMF-NO bound to unliganded (deoxygenated) Hb, while the hydrolyzed product, 5HMF bound to liganded (carbonmonoxy-ligated) Hb. Our findings from this proof-of-concept study suggest that the incorporation of NO donor group to 5HMF and analogous molecules could be a novel beneficial strategy to treat SCD and warrants further detailed in vivo studies.

Keywords: hemoglobin; sickle cell disease; antisickling; nitric oxide; oxygen equilibrium curve

1. Introduction

Sickle cell disease (SCD) occurs as a result of a single point mutation of β Glu6 in normal hemoglobin (HbA) to β Val6 in sickle hemoglobin (HbS), which leads to stereospecific interactions between deoxygenated HbS (deoxyHbS) molecules to form polymers, causing red blood cells (RBCs) to deform into rigid sickled cells [1–4]. This primary pathophysiology leads to a cascade of secondary adverse effects that include occlusion of rigid sickle RBCs in capillaries and small blood vessels and obstructing blood flow (vaso-occlusion), hemolytic anemia, hypoxia, stroke, and organ damage [5,6]. Sickled RBCs are also very fragile, leading to hemolysis and consequent release of free hemoglobin (Hb) into blood circulation. The free plasma Hb is a potent nitric oxide (NO) scavenger, and not only leads to NO deficiency but also results in the formation of reactive oxygen species, such as superoxide and peroxide radicals [7–10]. Furthermore, the enzyme arginase released from the hemolyzed RBCs

depletes plasma arginine levels. Arginine is an important source for NO production in the body by the enzyme NO synthase [11,12]. The ensuing deficiency of NO from the blood plasma leads to hypertension, inflammation; all common pathological conditions of SCD [13,14]. Four drugs, hydroxyurea, [15,16] Endari, [17] Crizanlizumab, [18] and Voxelotor [19–22] are currently approved for the treatment of SCD. While hydroxyurea has been used for over two decades, the other drugs were only recently approved. However, the inherent complexity of SCD suggests that none of the individual drugs are likely to universally be effective across patient populations, therefore the need remains for newer therapeutic options, particularly those that may incorporate more than one mechanism of action.

Hb is responsible for ensuring oxygen (O₂) distribution in the body by binding and transporting O₂ from the lungs to tissues. It carries out this function by equilibrating between the high-O₂-affinity relaxed state (R-state) and the low-O₂-affinity tense state (T-state). The relaxed or R-state is an ensemble of relaxed quaternary hemoglobin, which includes the classical R-state, R2-state, RR2-state, R3-state, etc. [23]. The O₂ affinity of Hb is denoted as P₅₀, the partial pressure of oxygen in mmHg, at which 50% of Hb is saturated with oxygen. Stabilization of deoxyHb or T-state Hb by allosteric effectors of Hb leads to an increase in the P₅₀ (decrease Hb affinity for oxygen) or shifts the oxygen equilibrium curve (OEC) to the right, which can be potentially useful for increasing tissue oxygenation [23]. On the other hand, stabilization of the R-state and/or destabilization of the T-state leads to a decrease in the P₅₀ (increase Hb affinity for oxygen) or shifts the OEC to the left [23]. Such compounds are potential antisickling agents since high-O₂-affinity HbS does not polymerize [23]. A number of aromatic aldehydes that bind and increase Hb affinity for oxygen have been studied by our group for their potential therapeutic application in SCD treatment [24–30]. These aldehydes form Schiff base adducts with the N-terminal α Val1 amines at the α -cleft of Hb to stabilize the R-state Hb and prevent hypoxia-induced HbS polymerization [24–30]. Voxelotor, is an example of aromatic aldehyde that was recently approved by the FDA in 2019 for the treatment of SCD [19–22]. Another example is 5-hydroxymethylfurfural (5HMF), a natural aromatic aldehyde that was studied in the clinic prior to Voxelotor discovery [25–27,31,32]. In vitro studies show that 5HMF formed an adduct with Hb (modified Hb), increased Hb affinity for oxygen, decreased HbS polymerization and RBC sickling, reduced sickle cell (SS) mechanical fragility, and reduced RBC hemolysis [25–27,31,32]. Under severe hypoxic conditions, 5HMF also significantly reduced the formation of sickled cells and prolonged the survival time of a SCD mouse model when administered orally [26]. 5HMF underwent phase I clinical trials for the treatment of SCD but failed to pass beyond Phase II trials, due in part to the unblinding of the study result and suboptimal pharmacokinetic properties [31,32].

Another treatment modality to mitigate SCD severity is to target the secondary pathophysiology of the disease with NO therapy. NO is an endothelium-derived relaxing factor (EDRF) that is highly involved in blood vessel dilatation and smooth muscle relaxation [33–35]. NO also modulates inflammation by inhibiting vascular remodeling [36]. NO is generated from L-arginine by NO synthase that is primarily found in the vascular endothelium, and from nitrite/nitrate by Hb and in the RBCs [37–39]. Deficiency of NO in blood plasma is one of the common pathological conditions in SCD that potentiates hemolysis, inflammation, vaso-occlusion (VOC), hypertension, oxidative stress, and tissue damage [13,40]. Inhaled NO therapy has been reported clinically to be useful in SCD patients [10,14,41,42]. In addition to inhalation of NO, long-lived circulating NO-releasing nanoparticles (NO-nps) and several NO-donor compounds, e.g., hydroxyurea, nitroglycerine, amyl nitrite, isosorbide dinitrate, NO-NSAIDs, nitrosothiols, nicorandil, sinitrodil, have been shown to have positive vasodilatory, anti-inflammatory and anti-hypertensive effects in SCD patients [43–47].

Based on the positive results of 5HMF as an antisickling agent and the potential benefits of providing exogenous NO in SCD patients, we decided to introduce NO releasing moiety to 5HMF with the aim of providing a novel approach for targeting several patholo-

gies of the disease. A NO releasing moiety was added to the methylhydroxyl of 5HMF to form a nitrate ester of 5HMF (5HMF-NO; Figure 1). 5HMF-NO was further evaluated in vitro for its ability to release NO, form adduct with Hb (Hb modification), increase Hb affinity for oxygen, prevent hypoxia-induced sickling, and finally for its atomic interaction with Hb.

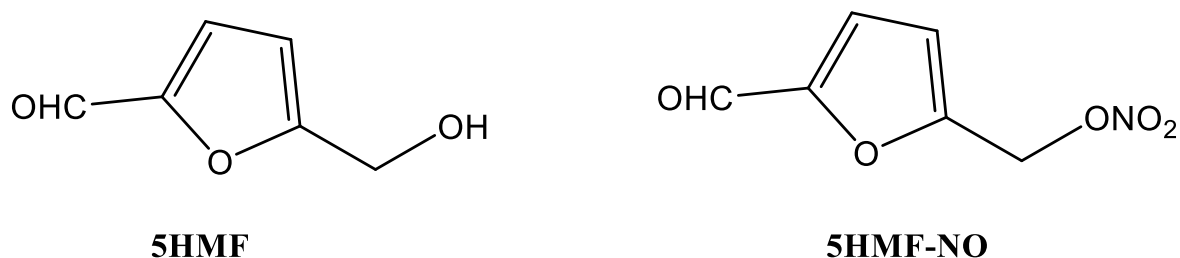


Figure 1. Structures of 5HMF and its NO-releasing derivative.

2. Materials and Method

2.1. Study Approvals

At Virginia Commonwealth University (VCU), normal whole blood (AA) was collected from adult donors (>18 years) after informed consent, in accordance with regulations of the IRB for Protection of Human Subjects (IRB #HM1) by the Institutional Review Board at VCU. At the Children's Hospital of Philadelphia (CHOP), leftover blood samples from individuals with homozygous sickle cell (SS) who had not been recently transfused, were obtained and utilized based on an approved IRB protocol (IRB# 11-008151) by the Institutional Review Board, with informed consent. All experimental protocols and methods were performed in accordance with institutional (VCU and CHOP) regulations. Hemoglobin for crystallographic studies was prepared as previously published [48,49].

2.2. Chemistry

All reagents used in the syntheses and functional assays were purchased from Sigma-Aldrich corporation and Fisher Scientific Company and used without purification. ¹H-NMR and ¹³C-NMR spectra were obtained on a Bruker 400 MHz spectrometer using tetramethylsilane (TMS) as an internal standard. Peak positions are given in parts per million (δ). Column chromatography was performed on silica gel (grade 60 mesh; Bodman Industries, Aston, PA, USA). Routine thin-layer chromatography (TLC) was performed on silica gel GHIF plates (250 μm, 2.5 × 10 cm; Analtech Inc., Newark, DE, USA). Elemental analysis was performed by Atlantic Microlab Inc. (Norcross, GA, USA) for the elements indicated and the results are within 0.4% of calculated values. Infrared spectra were obtained on a Thermo Nicolet iS10 FT-IR. Purity of the compounds was determined by HPLC using a Varian Microsorb 100-5 C18 column (250 × 4.6 mm), using Prostar 325 UV-Vis (254 nm) as the detector.

Synthesis of 5-Nitrooxymethyl Furfural (5HMF-NO)

5HMF-NO was prepared according to literature procedure for a similar compound [50]. Trifluoroacetic anhydride (5.5 mL, 2 mmol) was added to a suspension of lithium nitrate (2.7 g, 2 mmol) in anhydrous CH₃CN (30 mL) at 20 °C. The reaction mixture was stirred until clear (30 min) and cooled to 0 °C (ice-bath). Sodium carbonate (4.2 g, 2 mmol) and 5HMF (2.5 g, 1 mmol) were added together and the reaction mixture was allowed to stir for 7 h at 0 °C (ice-bath). The reaction mixture was poured into an ice-cold solution of saturated NaHCO₃ and extracted with EtOAc (2 × 10 mL). The combined organic portion was washed with brine (10 mL), dried over Na₂SO₄ and evaporated under reduced pressure to yield a crude product, which was purified by column chromatography (petroleum ether/EtOAc; 2:1) to afford 2.9 g (85%) of 5HMF-NO as a colorless viscous oil: IR (KBr, cm⁻¹): 1678 (C = O), 1631, 1276 (NO₂), 845 (ON); ¹H-NMR (CDCl₃): δ 5.48 (s, 2H, CH₂),

6.73 (d, $J = 3.5$ Hz, 1H, ArH), 7.25 (d, $J = 3.6$, 1H, ArH), 9.68 (s, 1H, CHO); ^{13}C -NMR (CDCl_3): δ 177.9, 153.4, 151.5, 120.9, 114.5, 65.4. Anal. Calcd for ($\text{C}_6\text{H}_5\text{NO}_5$) C, 42.12; H, 2.95; N, 8.19. Found: C, 42.02; H, 2.86; N, 8.26. The purity of the compound was checked by HPLC and found to be 98.8% pure.

2.3. Study of NO Release from 5HMF-NO in Whole Blood

The ability of 5HMF-NO to release the bound NO when incubated with whole blood was tested in a time-dependent manner using Griess assay as reported in the literature [51]. In this assay, whole blood from normal healthy individuals (adjusted to a hematocrit level of 30%) was mixed in 96-well plate (in duplicate or triplicate) with 5HMF-NO or 5HMF (control) to a final concentration of 1 mM and incubated in a shaker at 37 °C. Aliquots of blood were withdrawn at 0.5, 1, 2, 4, 6 and 18 h, and subsequently centrifuged (in a microcentrifuge) to separate out the plasma. To 50 μL of the separated plasma, 2.5 μL *Aspergillus* nitrate reductase (0.05 U), 0.25 μL FAD (5 μM) and 0.25 μL NADPH (0.1 mM) were added to convert nitrate to nitrite. 197 μL buffer (50 mM HEPES, PH 7.5) was added to adjust the volume to 250 μL . Next, the tubes were incubated at room temperature for 2 h. Then, 2.5 μL lactate dehydrogenase (2 mg/mL) and 25 μL Na pyruvate (100 mM stock) were added to consume leftover NADPH, and the tubes further incubated at room temperature for another 10 to 15 min. 50 μL of freshly mixed Griess reagent (Thermo Scientific, Waltham, MA, USA) was added to 125 μL of the reaction mixture, and the reaction volume was made to 1.5 mL distilled water. The tubes were then incubated in the dark for 30 min. The absorbance of the samples was read at 548 nm. Solutions of 0–100 μM sodium nitrite control solutions were used to generate the standard curve by a nitrite absorbance versus concentration under the same experimental conditions. Nitrite ion released by 5HMF-NO was calculated from the standard nitrite concentration curve.

2.4. In Vitro Hb Modification, Oxygen Equilibrium and Antisickling Studies Using Human Homozygous Sickle Cell (SS) Blood

5HMF-NO and the control 5HMF were studied for their abilities to modify Hb, increase Hb affinity for oxygen and inhibit hypoxia-induced RBC sickling (RBC morphology study) as previously described [26,27,30]. Briefly, SS blood (hematocrit of 20%) suspensions were incubated under air in the absence or presence of 1, 2 or 5 mM concentration of test compound at 37 °C for 1 h. Next, the suspensions were incubated under hypoxic condition (2.5% O_2 /97.5% N_2) at 37 °C for 2 h. Aliquot samples were fixed with 2% glutaraldehyde solution without exposure to air, and then subjected to microscopic morphological analysis. To determine whether 5HMF-NO retained the parent 5HMF's ability to form adduct and modify Hb, hemolysates from the above antisickling studies were subjected to a cation-exchange HPLC (Hitachi D-7000 Series, Hitachi Instruments, Inc., San Jose, CA, USA) using a weak cation-exchange column (Poly CAT A: 30 mm \times 4.6 mm, Poly LC, Inc., Columbia, MD, USA). Finally, for the oxygen equilibrium studies, 100 μL aliquot samples from the above clarified lysate were added to 4 mL of 0.1 M potassium phosphate buffer, pH 7.0, in cuvettes and subjected to hemoximetry analysis using a HemoxTM Analyzer (TCS Scientific Corp., New Hope, PA, USA) to determine the P_{50} values.

2.5. Crystallographic Study of Hb Co-Crystallized with 5HMF-NO

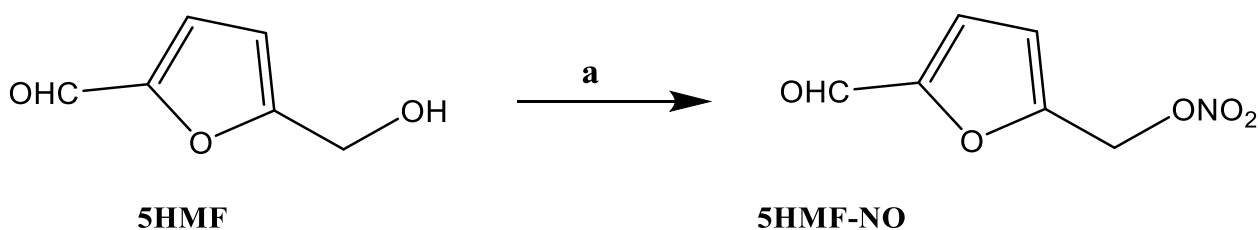
X-ray crystallography was performed to study the atomic interactions of 5HMF-NO with Hb, following the previously reported procedure [27,28]. For the crystallization experiment, 40 mg/mL of Hb was incubated with 20 molar excess of 5HMF-NO, and then evacuated for ~1 h to make the deoxyHb-compound complex solution. Next, sodium cyanoborohydride (NaCNBH_4) in 10 molar excess of Hb was added to reduce the reversible Schiff base adduct formed between the amino group of Hb and the aldehyde of 5HMF-NO to the corresponding irreversible alkylamine covalent bond. Subsequent crystallization of the deoxyHb-compound complex in test tubes using 3.2–3.6 M sulfate/phosphate precipitant pH 6.5, and ferrous citrate (50 μL) in a glovebox under nitrogen atmosphere led

to formation of two different crystal forms [27,28]. The crystals, corresponding to T-state and R2-state crystals were used for X-ray diffraction data collection at 100K using Rigaku MicroMax™ 007HF X-ray Generator, Eiger R 4M Detector and Oxford Cobra Cryo-system (The Woodlands, TX, USA). The crystals were first washed in a cryoprotectant solution containing 50 μ L mother liquor and 10–12 μ L glycerol prior to X-ray diffraction. The collected data sets were processed with the CrysAlisPro software program (Rigaku) and the CCP4 suite of programs [52]. The T-state and R2-state crystal structures were refined using the Phenix program with the previously reported isomorphous T-state and R2-state crystal structures (PDB ID: 2HHB and 1QXE), respectively, as starting models. Model building and correction were carried out using COOT [53–55]. The final Rfactor/Rfree of the T-state and R2-state structures are 15.1/19.1 and 18.6/22.8%, respectively.

3. Results and Discussion

3.1. Chemistry

In this study, we incorporated an NO-donor group onto the previously studied antisickling compound, 5HMF, to give the nitrate ester prodrug 5HMF-NO, as shown in Scheme 1. Briefly, 5HMF was nitrated directly using lithium nitrate and trifluoroacetic anhydride under basic conditions at zero degrees Celsius to give 5HMF-NO in 98.8% yield (Figure S1 in Supplementary Materials).



Scheme 1. 5HMF-NO. (a) LiNO_3 , TFAA, Na_2CO_3 , anhydrous CH_3CN , 0°C , 7 h.

3.2. 5HMF-NO Is Capable of Releasing NO

The key to the effectiveness of 5HMF-NO is its ability to release NO and the parent 5HMF for their respective beneficial effects. Griess assay was therefore used to measure the NO release from 5HMF-NO using human whole blood. Aliquots of the compounds incubated with the blood at 37°C were withdrawn at various time points (0.5, 1, 2, 4, 6 and 18 h), and plasma obtained from these samples was added to the Griess reagent to detect the released NO in the form of nitrite ion (NO_2^-). The nitrite release (nmol) was calculated from a standard NaNO_2 curve by extrapolating the absorbance (548 nm) of the Griess reagent-nitrite azo dye complex against the concentration of NaNO_2 . Results, expressed as the concentration of nitrite versus time (Table 1 and Figure 2) show that 5HMF-NO was able to release nitrite over the course of the experiment, while, the control group (5HMF or absence of compound) exhibited no formation of nitrite. There is a quick release of 9.4 nmol nitrite at 0.5 h, which slightly increased to about 11 nmol at two hours, and then sustained throughout the 18-h experiment. We expect a similar release of 5HMF and NO in vivo, although the amount and mode of NO release could be different. Based on the previously proposed mechanism of biotransformation of NO-releasing prodrugs from nitrate ester groups, [46,51,56] we expect the release of the NO to involve both enzymatic action and chemical hydrolysis. A potential pharmacologic disadvantage of 5HMF-NO is that its use could lead to clinical nitrate tolerance development, especially if the NO-release is dependent on metabolic activation that decreases in efficiency upon continued use [46,57].

Table 1. NO release from 5HMF-NO in human whole blood.

Compound	NO ₂ ⁻ Concentration (nmol)					
	0.5 h	1 h	2 h	4 h	6 h	18 h
5HMF-NO	9.44 ± 0.63	10.1 ± 0.97	10.6 ± 1.19	9.98 ± 1.11	10.8 ± 1.03	10.9 ± 0.91
5HMF	0.00 ± 0.00	0.59 ± 0.01	0.73 ± 0.01	0.73 ± 0.01	0.30 ± 0.02	0.079 ± 0.00
Control	0.00 ± 0.04	0.42 ± 0.00	0.04 ± 0.28	0.66 ± 0.00	0.00 ± 0.52	1.18 ± 0.52

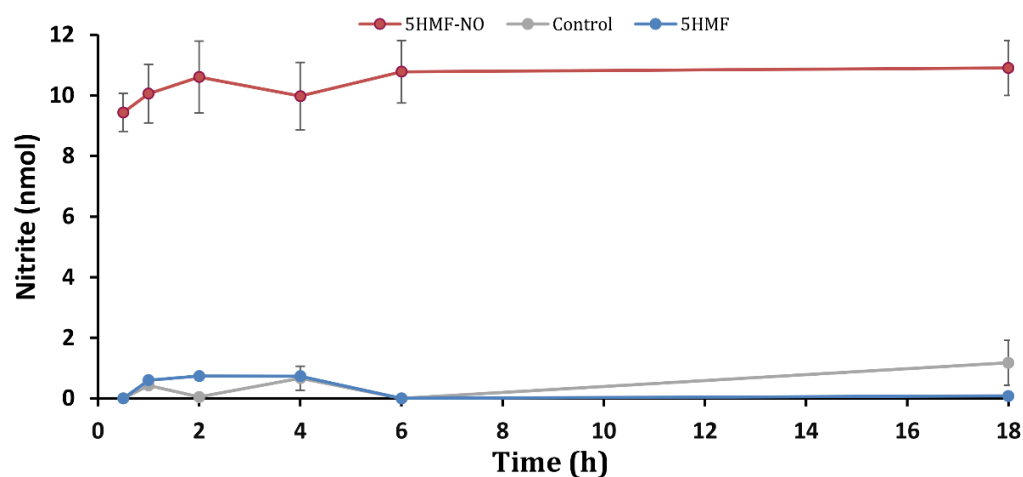


Figure 2. Time-dependent NO release from 5HMF-NO. NO release (in the form of nitrite) by 5HMF-NO (red), 5HMF (cyan), and no test compound (grey). The results are the mean values ± SD for biological duplicate or triplicate experiments. All compounds were solubilized in 2% DMSO. Control experiment without test compound also included 2% DMSO. Final test compound concentration was 1 mM.

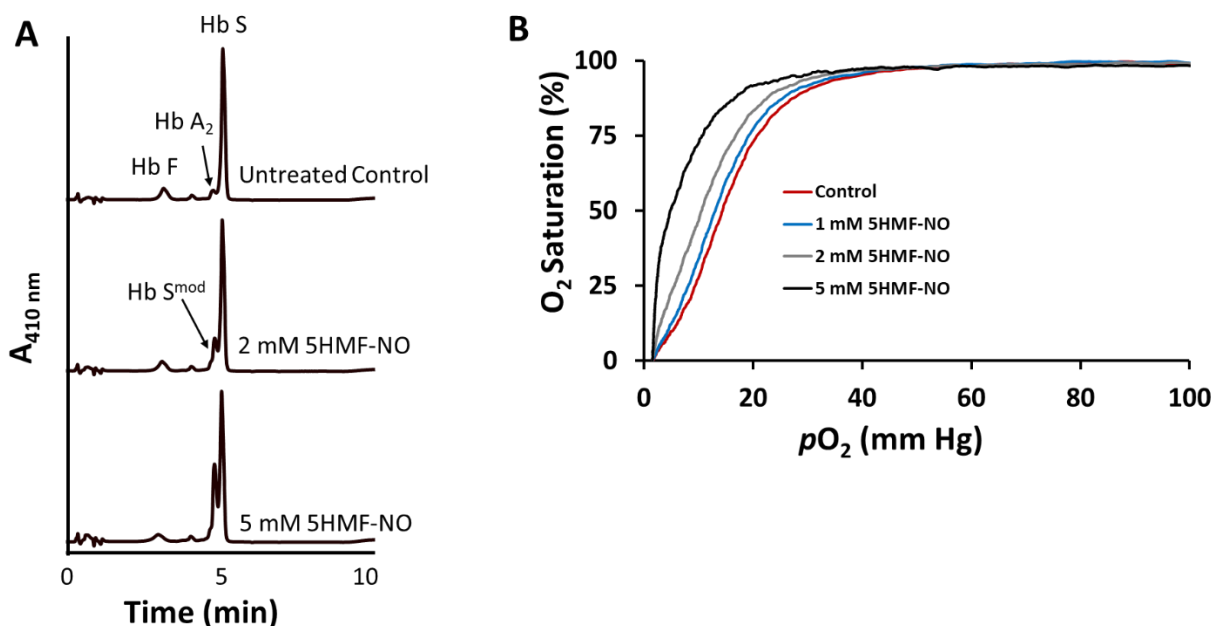
The NO release in the form of nitrite (nmol) was calculated from a standard NaNO₂ curve by extrapolating the absorbance (548 nm) of the Griess reagent-nitrite azo dye complex. The results are the mean values ± SD for biological duplicate or triplicate experiments. All compounds were solubilized in 2% DMSO. The final test compound concentration is 1 mM. The control experiments without a test compound also included 2% DMSO.

3.3. 5HMF-NO Forms Adduct with Hb to Increase the Affinity of Hb for Oxygen and Prevent Hypoxia-Induced RBC Sickling

This study was conducted to determine the extent of Hb modification and antisickling activities of 5HMF-NO using SS blood and to correlate the result with its allosteric activity of modulating Hb oxygen binding properties. 5HMF-NO and the positive control 5HMF were dose-dependently (1, 2, and 5 mM) incubated with whole SS blood suspensions (hematocrit of 20%) under hypoxic conditions (2.5% O₂/97.5% N₂) at 37 °C for 2 h to form adduct with Hb. Aliquot blood samples were drawn and used for assessing RBC morphology, Hb affinity for oxygen and Hb adduct formation as previously described [26,27,29,30]. The results summarized in Table 2 and Figures 3 and 4 show dose-dependent effects for all three pharmacodynamic parameters, and expectedly show direct correlation among them. 5HMF-NO modified Hb by 16%, 21% and 38% at 1 mM, 2 mM and 5 mM, respectively (compared to 21%, 31% and 54% by 5HMF), increase Hb affinity for oxygen (P₅₀-shift) by 10%, 27%, and 67% (compared to 18%, 33%, and 54% by 5HMF), translating into RBC sickling inhibition of 27%, 39% and 60% (compared to 21%, 50% and 69% by 5HMF). It is clear that 5HMF-NO maintains the pharmacodynamic activities of 5HMF.

Table 2. Hemoglobin modification, change in oxygen equilibrium, and antisickling studies of 5HMF and 5HMF-NO using human sickle blood.

Compound	% Functional/Biological Effect								
	Hb Modification			Sickling Inhibition			ΔP_{50}		
	1 mM	2 mM	5 mM	1 mM	2 mM	5 mM	1 mM	2 mM	5 mM
5HMF-NO	15.9 ± 0.2	20.7 ± 1.3	38.1 ± 0.6	27.0 ± 8.4	38.9 ± 15.1	59.9 ± 8.2	10.0	27.2	66.9
5HMF	21.1 ± 0.6	30.9 ± 1.7	53.7 ± 0.1	20.6 ± 4.2	49.7 ± 4.8	68.5 ± 2.3	18.4	33.0	53.9

**Figure 3.** Representative figures of Hb modification and OEC shift by 5HMF-NO in sickle blood: (A) Cation exchange HPLC chromatograms showing a dose-dependent Hb modification; (B) OEC curves demonstrating a doses-dependent left-shift in oxygen affinity study.

The results are the mean values \pm SD for two or three biological replicate experiments for the Hb modification and antisickling studies, and single measurement for the OEC study. The differences between the 5HMF and the 5HMF-NO groups were not statistically significant (p values of 0.2, 0.66, and 0.98, respectively). All compounds were solubilized in DMSO (2%). The control experiments without a test compound also contain 2% DMSO.

$$\Delta P_{50} (\%) = \frac{P_{50} \text{ of lysates from untreated cells} - P_{50} \text{ of lysates from treated cells}}{P_{50} \text{ of lysates from untreated cells}} \times 100$$

3.4. 5HMF-NO When Co-Crystallized with Hb Binds to the T-State as 5HMF-NO and R2-State Hb as 5HMF

An X-ray crystallographic study was performed to help gain insight into the mechanism of action of 5HMF-NO, and detailed crystallographic data for the reported structures are shown in Table 3. As previously reported for several aromatic aldehydes, [27,28] deoxyHb when co-crystallized with 5HMF-NO resulted in two different crystal forms: dark purple rectangular-shaped T-state crystals that appeared within 2–4 days, followed by reddish trigonal-shaped R2-state crystals that appeared about four weeks later. Expectedly, the crystal parameters and eventually the corresponding structures are isomorphous to T-state (PDB 2HHB) and R2-state (PDB 1BBB) structures, respectively (Table 3). Aromatic aldehydes are known to preferentially bind to the relaxed R2-state conformation to increase Hb affinity for oxygen [23,27,28,58].

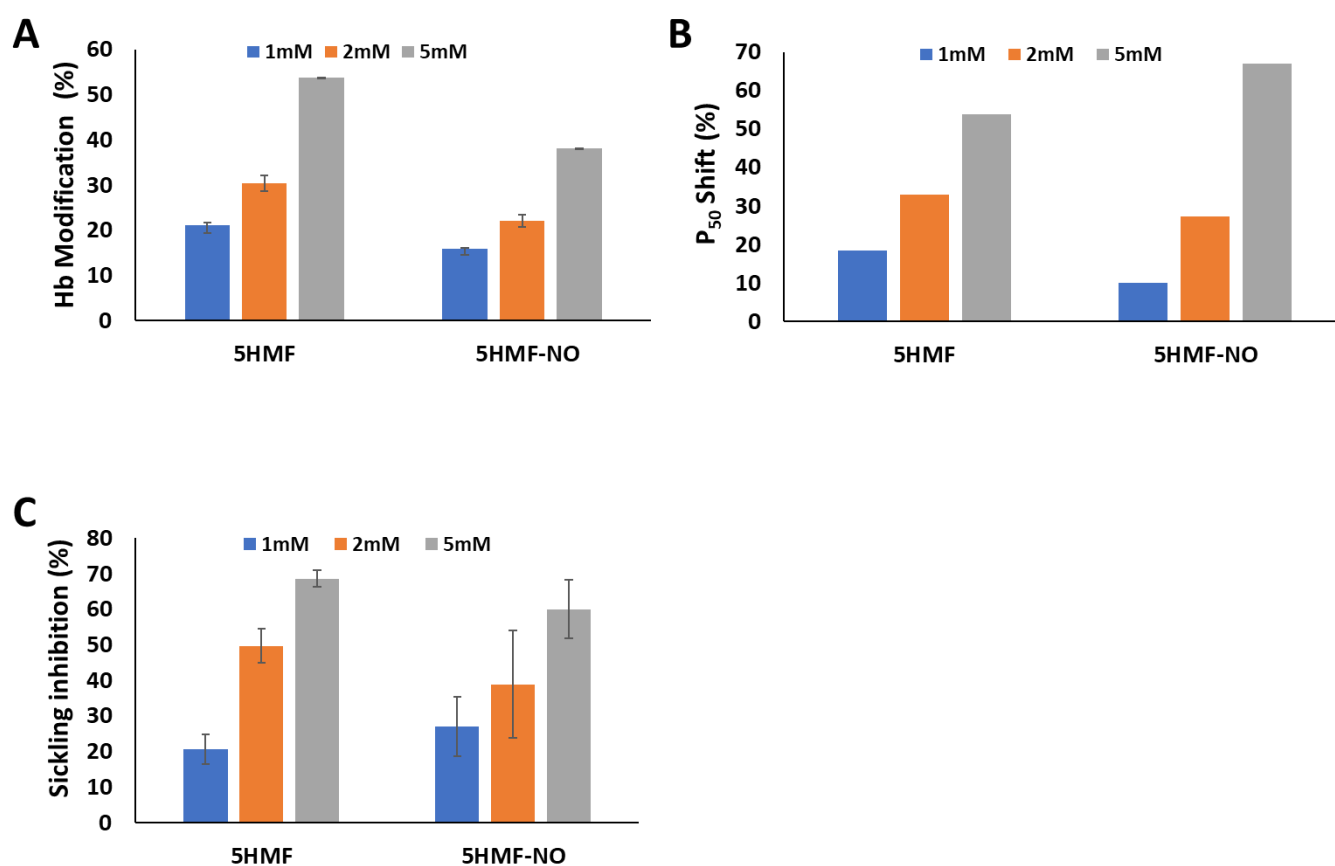


Figure 4. Functional/biological effects of 5HMF-NO in sickle blood. Hb modification, oxygen equilibrium and antisickling studies were conducted with SS blood suspensions (hematocrit of 20%) incubated with 1, 2 and 5 mM of 5HMF or 5HMF-NO. The final concentration of DMSO was <2% in all samples, including in control samples. The results are the mean values \pm SD for two or three biological replicate experiments for the Hb modification and antisickling studies, and single measurement for the OEC study. The differences between the 5HMF and the 5HMF-NO groups were not statistically significant (p values of 0.2, 0.66, and 0.98, respectively). (A) Concentration-dependent modification of Hb S; (B) Concentration-dependent P_{50} shift of Hb S; (C) Concentration-dependent inhibition of SS cell sickling under hypoxia.

The T-state Hb or R2-state Hb structure showed two compounds bound at the α -cleft; the molecules forming Schiff base interactions with α Val1 amines of both α 1- and α 2-subunits in a symmetry-related fashion. Interestingly, while the T-state Hb binds the prodrug 5HMF-NO, the R2-state Hb binds the hydrolyzed product 5HMF (Figures 5 and 6). It is clear that hydrolysis of the nitrate ester might have occurred during crystallization to release some 5HMF, which then bound to deoxygenated Hb. Similar chemical hydrolysis of the organic molecule nitrate esters to release NO, and crystallization has been reported [51]. Expectedly, the T-state Hb structure lacks oxygen at the hemes, while the R2-state Hb structure shows bound oxygen atoms at all four hemes, presumably from residual or slow diffusion of oxygen into the crystallization tube, as previously reported [27,28]. The root mean square deviation (Rmsd) between the R2-state Hb complex structure and the previously reported liganded R2-state Hb structure (PDB code IBBB) [59] or the T-state Hb complex structure and the previously reported unliganded T-state Hb structure (PDB code 2HHB) [60] is ~ 0.4 Å, suggesting that binding of the molecules to the respective quaternary structures does not induce any significant conformational changes.

Table 3. Crystallographic data and refinement statistics for unliganded (T-state) Hb in complex with 5HMF-NO and liganded (R2-state) Hb in complex with 5HMF.

Data Collection Statistics	5HMF-NO (T-State)	Hydrolyzed 5HMF (R2-State)
PDB ID	7UD7	7UD8
Space group	P2 ₁	P3 ₂ 21
Cell dimensions (Å)	62.34, 82.03, 53.45; 99.49	92.23, 92.23, 144.07
Tetramer/AU	1	1
Resolution (Å)	29.92–1.80 (1.86–1.80)	28.39–1.80 (1.84–1.80)
Measured reflections	18,7917	71,6379 (20,836)
Unique reflections	46,300 (4367)	66,309 (3896)
Redundancy	4.06 (3.81)	10.8 (5.3)
I/σI	25.9 (10.8)	28.8 (2.0)
Completeness (%)	94.1 (89.4)	100 (99.7)
R _{merge} (%) ^a	3.9 (8.2)	5.5 (72.7)
Structure refinement		
Resolution limit (Å)	26.36–1.80 (1.86–1.80)	28.39–1.80 (1.86–1.80)
No. of reflections	46,299 (4366)	66,260 (6521)
R _{work} (%)	15.1 (18.9)	18.6 (24.1)
R _{free} (%) ^b	19.1 (24.4)	22.8 (26.9)
Rmsd geometry		
Bond lengths (Å)	0.007	0.026
Bond angles (°)	1.37°	2.01°
Dihedral angles (%)		
Most favored regions	98.2	98.1
Allowed regions	1.6	1.6
Average B-factors (Å²)		
All atoms	15.6	27.3
Protein alone	13.84	26.2
Ligands	13.74	24.5
Water	26.18	35.4

^a R_{merge} = $\sum_{hkl} \sum_i |I_{hkl} - \langle I_{hkl} \rangle| / \sum_{hkl} \sum_i \langle I_{hkl} \rangle$. ^b R_{free} was calculated with 5% excluded reflection from the refinement.

The bound 5HMF molecules in the R2-state Hb structure is similar to the previously reported R2-state Hb structure in complex with 5HMF (PDB code 1QXE) [27]. In addition to the Schiff base interaction with the αVal1 amine of the α-subunits, 5HMF makes several intra- and inter-subunit protein interactions. At the α1-subunit binding site, the furan ring oxygen and the methylhydroxyl moiety of 5HMF engage in intra-subunit hydrogen-bond interactions with α1Ser131 OG (3.2 Å) and α1Thr134 OG1 (2.6 Å), respectively (Figure 5). Similar symmetry-related interactions by the second molecule are observed at the α2-subunit. Additionally, the two bound 5HMF molecules are joined together, and to the protein by a network of several inter-subunit and intra-subunit water-mediated hydrogen-bond interactions, through the methylhydroxyl and the furan ring oxygen moieties (Figure 5). These interactions, as previously noted, [27] serve to tie the two α-subunits together, and expected to stabilize the relaxed state Hb, explaining the compound's ability to increase Hb affinity for oxygen with a concomitant antisickling effect.

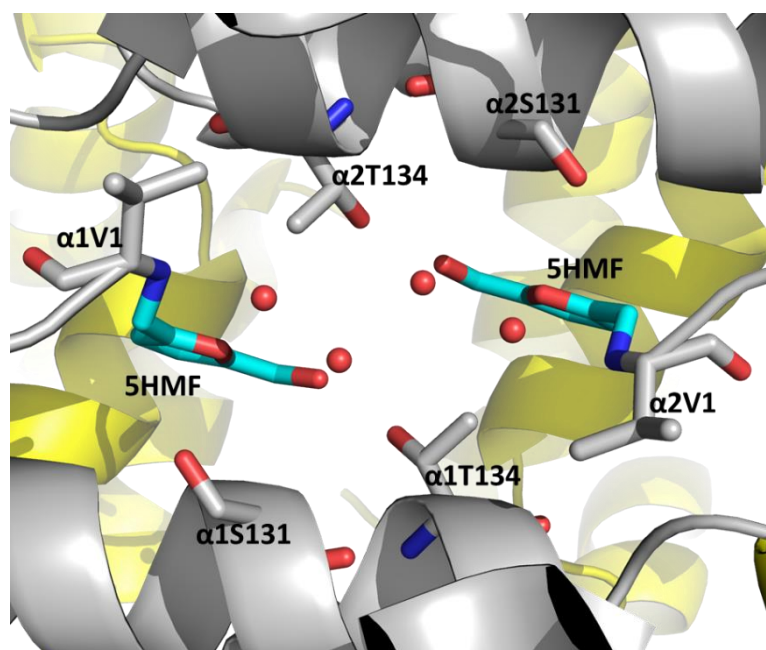


Figure 5. Binding of a pair of 5HMF molecules (cyan sticks) at the α -cleft of R2-state Hb. The α -chain (α_1 - and α_2 -subunits) colored in grey and β -chain (β_1 - and β_2 -subunits) colored in yellow. Water molecules are red spheres.

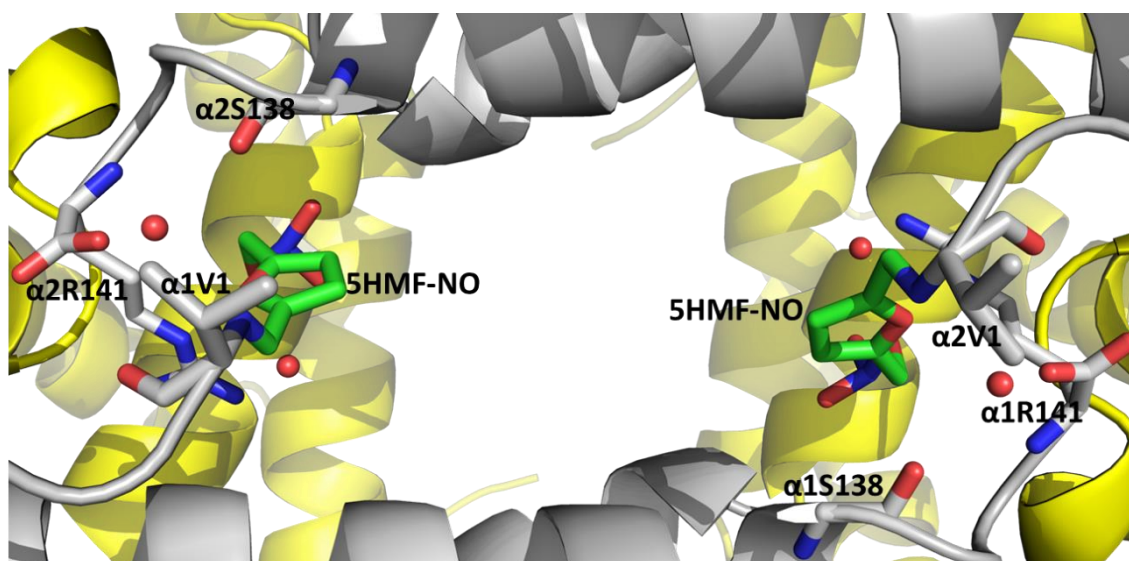


Figure 6. Binding of a pair of 5HMF-NO molecules (green sticks) at the α -cleft of T-state Hb. The α -chain (α_1 - and α_2 -subunits) colored in grey and β -chain (β_1 - and β_2 -subunits) colored in yellow. Water molecules are red spheres.

Unlike the R2-state Hb structure that binds 5HMF, the T-state Hb interestingly binds 5HMF-NO. In addition to the Schiff base interaction by 5HMF-NO with the α_2 -subunit α_2 Val1 amine, the furan oxygen forms inter-subunit water-mediated hydrogen-bond interactions with the amide oxygen of α_1 Ser138 and the carboxyl atom of α_1 Arg141 (Figure 6). The ester oxygen atom and one of the nitro oxygen atoms of 5HMF-NO make inter-subunit hydrogen-bond interactions with the guanidinium group of α_1 Arg141 (3.2 Å and 3.3 Å, respectively). There is also an inter-subunit water-mediated hydrogen-bond interaction between the ester oxygen atom and the guanidinium group of α_1 Arg141. The nitro group oxygen also makes direct inter-subunit hydrogen-bond interaction with the amide of α_1 Thr137 (3.4 Å). The second 5HMF-NO molecule forms a Schiff-base interaction with the

α 1-subunit α 1Val1 amine and makes similar symmetry-related interactions with the protein as described above for the first 5HMF-NO molecule at the α 2Val1 binding site, although in some instances with slightly different bond distances. The interactions by 5HMF-NO are expected to stabilize the T-state Hb and restrict the transition to the R-state.

It is interesting that, in the R2 structure, the furan oxygen of 5HMF faces the central water cavity to make an intra-subunit hydrogen-bond interaction with α Ser131 OG, as well as water-mediated interactions with the protein, while in the T-state the furan ring of 5HMF-NO has rotated $\sim 180^\circ$ such that the oxygen makes an inter-subunit interaction with the guanidinium group of α Arg141. Furthermore, notably, unlike the R2-state structure where 5HMF mediates both inter-subunit and intra-subunit interactions with the protein, in the T-state structure, all the hydrogen-bond interactions are inter-subunit in nature. The $T \leftrightarrow R$ allosteric transition is known to lead to significant rearrangement of the α 1-subunit position relative to the α 2-subunit, resulting in a much larger central water cavity in the T-state Hb compared to the R2-state Hb. Consequently, the two 5HMF-NO molecules in the T structure are separated by 11.7 Å without any contact between the molecules. In contrast, the two bound 5HMF molecules in the R2 structure are only separated by 4.3 Å, interacting together through several water-mediated hydrogen-bond interactions.

It is clear that unlike 5HMF that binds to Hb and stabilizes the R2-state Hb, the binding of 5HMF-NO leads to the stabilization of T-state Hb. As previously noted, [23,58,61] the apparent stabilization of T-state Hb by 5HMF-NO is expected to lead to a decrease in Hb affinity for oxygen, which is clearly opposite to our observation of increased Hb affinity for oxygen when 5HMF-NO was tested with whole blood. It thus appears that in whole blood, there is significant hydrolysis of the ester nitrate to form 5HMF. It is assumed that in vivo, and particularly in the RBC, 5HMF-NO will exist predominantly as 5HMF, otherwise any significant amount of unhydrolyzed 5HMF-NO in the RBC could have a negative impact on sickling.

4. Conclusions

5HMF has previously been studied in the clinic for the treatment of SCD as a result of its ability to stabilize the high-O₂-affinity R-state Hb, and increase the concentration of the non-polymerizing oxygenated HbS [26,27]. We have synthesized NO-releasing prodrug of 5HMF (5HMF-NO) that is expected to be bio-transformed into 5HMF and NO in vivo and exhibit therapeutic activities. It is expected that controlled delivery of therapeutic quantities of NO—concurrently with 5HMF's primary antipolymerization properties—will ameliorate both primary and secondary pathophysiologic effects, including RBC sickling and hemolysis, inflammation, oxidative stress, painful VOC, and chronic organ damage. Our in vitro functional and biological analyses showed that 5HMF-NO is capable of hydrolyzing to release NO and 5HMF to increase the affinity of Hb for oxygen with a concomitant antisickling effect. Although, not studied for its pharmacologic effect, we expect the released NO to have a beneficial effect, and future studies will test this hypothesis.

Supplementary Materials: The following supporting information can be downloaded at: <https://www.mdpi.com/article/10.3390/biom12050696/s1>, Figure S1: HPLC Chromatogram of 5HMF-NO.

Author Contributions: O.A., Y.Z., and M.K.S. contributed to study conception. B.H., R.D.-D. and T.M.D. synthesized 5HMF-NO. O.A., N.A., M.S.G., D.A. and R.T.A. performed biochemical experiments. F.N.M., R.T.A. and A.K.D. crystallized and determined the crystal structures. O.A., Y.Z. and M.K.S. analyzed and interpreted data. M.S.G., R.T.A., T.M.D., O.A., M.K.S. wrote the manuscript. All authors provided final approval of the manuscript. All authors have read and agreed to the published version of the manuscript.

Funding: This work was supported by NIH/NIMHD grant R01MD009124 (M.K.S.) and NIH/NHLBI grant R61HL156158 (M.K.S. and O.A.). Structure biology resources were provided by NIH Shared Instrumentation Grant S10OD021756 (M.K.S.) and Virginia General Assembly Higher Education Equipment Trust Fund (HEETF) to Virginia Commonwealth University (M.K.S.).

Institutional Review Board Statement: The study was conducted in accordance with the Declaration of Helsinki, and approved by the Institutional Review Board (or Ethics Committee) of Virginia Commonwealth University (protocol code IRB #HM1; 10/27/2021) and the Children’s Hospital of Philadelphia (protocol code IRB# 11-008151; 9/27/2021) for studies involving humans.

Informed Consent Statement: Informed consent was obtained from all subjects involved in the study.

Data Availability Statement: The atomic coordinates and the structure factor of 5HMF-NO and 5HMF with Hb are deposited in the RCSB Protein Databank (<https://www.rcsb.org/>, accessed on 3 April 2022) with entries 7UD7 and 7UD8, respectively.

Conflicts of Interest: The authors declare no conflict of interest.

Abbreviations

Hb, hemoglobin; HbS, sickle hemoglobin; OEC, oxygen equilibrium curve; RBC, red blood cell; SCD, sickle cell disease; deoxyHb, deoxygenated hemoglobin; NO, nitric oxide; R-state or R2-state, relaxed state; T-state, tense state; 5HMF, 5-hydroxymethylfurfural; PO₂, partial pressure; SO₂, oxygen saturation; O₂, oxygen.

References

1. Pauling, L.; Itano, H.A.; Singer, S.J.; Wells, I.C. Sickle cell anemia, a molecular disease. *Science* **1949**, *110*, 543–548. [[CrossRef](#)] [[PubMed](#)]
2. Ghatge, M.S.; Ahmed, M.H.; Omar, A.S.M.; Pagare, P.P.; Rosef, S.; Kellogg, G.E.; Abdulmalik, O.; Safo, M.K. Crystal structure of carbonmonoxy sickle hemoglobin in R-state conformation. *J. Struct. Biol.* **2016**, *194*, 446–450. [[CrossRef](#)] [[PubMed](#)]
3. Cretegnny, I.; Edelstein, S.J. Double strand packing in hemoglobin S fibers. *J. Mol. Biol.* **1993**, *230*, 733–738. [[CrossRef](#)] [[PubMed](#)]
4. Ferrone, F.A. Polymerization and sickle cell disease: A molecular view. *Microcirculation* **2004**, *11*, 115–128. [[CrossRef](#)]
5. Thein, M.S.; Igbineweka, N.E.; Thein, S.L. Sickle cell disease in the older adult. *Pathology* **2017**, *49*, 1–9. [[CrossRef](#)]
6. Chaturvedi, S.; DeBaun, M.R. Evolution of sickle cell disease from a life-threatening disease of children to a chronic disease of adults: The last 40 years. *Am. J. Hematol.* **2016**, *91*, 5–14. [[CrossRef](#)]
7. Jin, R.C.; Loscalzo, J. Vascular nitric oxide: Formation and function. *J. Blood Med.* **2010**, *1*, 147.
8. Mack, A.K.; Kato, G.J. Sickle cell disease and nitric oxide: A paradigm shift? *Int. J. Biochem. Cell Biol.* **2006**, *38*, 1237–1243. [[CrossRef](#)]
9. Kassim, A.A.; DeBaun, M.R. Sickle cell disease, vasculopathy, and therapeutics. *Annu. Rev. Med.* **2013**, *64*, 451–466. [[CrossRef](#)]
10. Head, C.A.; Brugnara, C.; Martinez-Ruiz, R.; Kacmarek, R.M.; Bridges, K.R.; Kuter, D.; Bloch, K.D.; Zapol, W.M. Low concentrations of nitric oxide increase oxygen affinity of sickle erythrocytes in vitro and in vivo. *J. Clin. Investig.* **1997**, *100*, 1193–1198. [[CrossRef](#)]
11. Steppan, J.; Tran, H.T.; Bead, V.R.; Oh, Y.J.; Sikka, G.; Bivalacqua, T.J.; Burnett, A.L.; Berkowitz, D.E.; Santhanam, L. Arginase inhibition reverses endothelial dysfunction, pulmonary hypertension and vascular stiffness in transgenic sickle cell mice. *Anesth. Analg.* **2016**, *123*, 652. [[CrossRef](#)]
12. Iyamu, E.W.; Cecil, R.; Parkin, L.; Woods, G.; Ohene-Frempong, K.; Asakura, T. Modulation of erythrocyte arginase activity in sickle cell disease patients during hydroxyurea therapy. *Br. J. Haematol.* **2005**, *131*, 389–394. [[CrossRef](#)]
13. Kahn, M.J.; Maley, J.H.; Lasker, G.F.; Kadowitz, P.J. Updated role of nitric oxide in disorders of erythrocyte function. *Cardiovasc. Haematol. Disord. Drug Targets* **2013**, *13*, 83–87. [[CrossRef](#)]
14. Kim-Shapiro, D.B.; Gladwin, M.T. Nitric oxide pathology and therapeutics in sickle cell disease. *Clin. Hemorheol. Microcirc.* **2018**, *68*, 223–237. [[CrossRef](#)]
15. Mvalo, T.; Topazian, H.; Kamthunzi, P.; Chen, J.; Kambalame, I.; Mafunga, P.; Mumba, N.; Chiume-Chiphaliwali, M.; Paseli, K.; Key, N. Increasing hydroxyurea use in children with sickle cell disease at Kamuzu Central Hospital, Malawi. *Blood Adv.* **2018**, *2*, 30. [[CrossRef](#)]
16. Zhu, X.; Hu, T.; Ho, M.H.; Wang, Y.; Yu, M.; Patel, N.; Pi, W.; Choi, J.-H.; Xu, H.; Ganapathy, V. Hydroxyurea differentially modulates activator and repressors of γ -globin gene in erythroblasts of responsive and non-responsive patients with sickle cell disease in correlation with Index of Hydroxyurea Responsiveness. *Haematologica* **2017**, *102*, 1995. [[CrossRef](#)]
17. L-glutamine (Endari) for sickle cell disease. *Med. Lett. Drugs Ther.* **2018**, *60*, 21–22.
18. Ataga, K.I.; Kutlar, A.; Kanter, J.; Liles, D.; Cancado, R.; Friedrisch, J.; Guthrie, T.H.; Knight-Madden, J.; Alvarez, O.A.; Gordeuk, V.R. Crizanlizumab for the prevention of pain crises in sickle cell disease. *N. Engl. J. Med.* **2017**, *376*, 429–439. [[CrossRef](#)]
19. Hutchaleelaha, A.; Patel, M.; Silva, A.; Oksenberg, D.; Metcalf, B. GBT440 demonstrates high specificity for red blood cells in nonclinical species. *Blood* **2015**, *126*, 2172. [[CrossRef](#)]

20. Metcalf, B.; Chuang, C.; Dufu, K.; Patel, M.P.; Silva-Garcia, A.; Johnson, C.; Lu, Q.; Partridge, J.R.; Patskovska, L.; Patskovsky, Y. Discovery of GBT440, an orally bioavailable R-state stabilizer of sickle cell hemoglobin. *ACS Med. Chem. Lett.* **2017**, *8*, 321–326. [[CrossRef](#)]
21. Oksenberg, D.; Dufu, K.; Patel, M.P.; Chuang, C.; Li, Z.; Xu, Q.; Silva-Garcia, A.; Zhou, C.; Hutchaleelaha, A.; Patskovska, L. GBT 440 increases haemoglobin oxygen affinity, reduces sickling and prolongs RBC half-life in a murine model of sickle cell disease. *Br. J. Haematol.* **2016**, *175*, 141–153. [[CrossRef](#)]
22. Vichinsky, E.; Hoppe, C.C.; Ataga, K.I.; Ware, R.E.; Nduba, V.; El-Beshlawy, A.; Hassab, H.; Achebe, M.M.; Alkindi, S.; Brown, R.C.; et al. A Phase 3 Randomized Trial of Voxelotor in Sickle Cell Disease. *N. Engl. J. Med.* **2019**, *381*, 509–519. [[CrossRef](#)]
23. Safo, M.K.; Ahmed, M.H.; Ghatge, M.S.; Boyiri, T. Hemoglobin–ligand binding: Understanding Hb function and allostery on atomic level. *Biochim. Biophys. Acta* **2011**, *1814*, 797–809. [[CrossRef](#)] [[PubMed](#)]
24. Nnamani, I.N.; Joshi, G.S.; Danso-Danquah, R.; Abdulmalik, O.; Asakura, T.; Abraham, D.J.; Safo, M.K. Pyridyl derivatives of benzaldehyde as potential antisickling agents. *Chem. Biodivers.* **2008**, *5*, 1762–1769. [[CrossRef](#)]
25. Oder, E.; Safo, M.K.; Abdulmalik, O.; Kato, G.J. New developments in anti-sickling agents: Can drugs directly prevent the polymerization of sickle haemoglobin in vivo? *Br. J. Haematol.* **2016**, *175*, 24–30. [[CrossRef](#)]
26. Abdulmalik, O.; Safo, M.K.; Chen, Q.; Yang, J.; Brugnara, C.; Ohene-Frempong, K.; Abraham, D.J.; Asakura, T. 5-hydroxymethyl-2-furfural modifies intracellular sickle haemoglobin and inhibits sickling of red blood cells. *Br. J. Haematol.* **2005**, *128*, 552–561. [[CrossRef](#)]
27. Safo, M.K.; Abdulmalik, O.; Danso-Danquah, R.; Burnett, J.C.; Nokuri, S.; Joshi, G.S.; Musayev, F.N.; Asakura, T.; Abraham, D.J. Structural basis for the potent antisickling effect of a novel class of five-membered heterocyclic aldehydic compounds. *J. Med. Chem.* **2004**, *47*, 4665–4676. [[CrossRef](#)]
28. Abdulmalik, O.; Ghatge, M.S.; Musayev, F.N.; Parikh, A.; Chen, Q.; Yang, J.; Nnamani, I.; Danso-Danquah, R.; Eseonu, D.N.; Asakura, T. Crystallographic analysis of human hemoglobin elucidates the structural basis of the potent and dual antisickling activity of pyridyl derivatives of vanillin. *Acta Crystallogr. D Biol. Crystallogr.* **2011**, *67*, 920–928. [[CrossRef](#)]
29. Abdulmalik, O.; Pagare, P.P.; Huang, B.; Xu, G.G.; Ghatge, M.S.; Xu, X.; Chen, Q.; Anabaraonye, N.; Musayev, F.N.; Omar, A.M.; et al. VZHE-039, a novel antisickling agent that prevents erythrocyte sickling under both hypoxic and anoxic conditions. *Sci. Rep.* **2020**, *10*, 20277. [[CrossRef](#)]
30. Pagare, P.P.; Ghatge, M.S.; Musayev, F.N.; Deshpande, T.M.; Chen, Q.; Braxton, C.; Kim, S.; Venitz, J.; Zhang, Y.; Abdulmalik, O. Rational design of pyridyl derivatives of vanillin for the treatment of sickle cell disease. *Bioorg. Med. Chem.* **2018**, *26*, 2530–2538. [[CrossRef](#)]
31. Stern, W.; Mathews, D.; McKew, J.; Shen, X.; Kato, G.J. A phase 1, first-in-man, dose–response study of Aes-103 (5-HMF), an anti-sickling, allosteric modifier of hemoglobin oxygen affinity in healthy normal volunteers. *Blood* **2012**, *120*, 3210. [[CrossRef](#)]
32. Safo, M.K.; Aljahdali, A.; Burnett, J.; Abraham, D.J.; Abdulmalik, O. Therapeutic Strategies for the Treatment of Sickle Cell Disease. In *Burger's Medicinal Chemistry and Drug Discovery*; John Wiley & Sons: Hoboken, NJ, USA, 2021; pp. 1–31.
33. Wong, G.; Marsden, P. Nitric oxide synthases: Regulation in disease. *Nephrol. Dial. Transplant.* **1996**, *11*, 215–220. [[CrossRef](#)] [[PubMed](#)]
34. Lamas, S.; Pérez-Sala, D.; Moncada, S. Nitric oxide: From discovery to the clinic. *Trends Pharmacol. Sci.* **1998**, *19*, 436–438. [[CrossRef](#)]
35. Ignarro, L.J. Nitric oxide: A unique endogenous signaling molecule in vascular biology. *Biosci. Rep.* **1999**, *19*, 51–71. [[CrossRef](#)]
36. De Franceschi, L. Pathophysiology of sickle cell disease and new drugs for the treatment. *Mediterr. J. Hematol. Infect. Dis.* **2009**, *1*, e2009024. [[CrossRef](#)]
37. Wallis, J. Nitric oxide and blood: A review. *Trans. Med.* **2005**, *15*, 1–11. [[CrossRef](#)]
38. Liu, C.; Wajih, N.; Liu, X.; Basu, S.; Janes, J.; Marvel, M.; Keggi, C.; Helms, C.C.; Lee, A.N.; Belanger, A.M. Mechanisms of human erythrocytic bioactivation of nitrite. *J. Biol. Chem.* **2015**, *290*, 1281–1294. [[CrossRef](#)]
39. Lundberg, J.O.; Weitzberg, E. NO generation from nitrite and its role in vascular control. *Arterioscler. Thromb. Vasc. Biol.* **2005**, *25*, 915–922. [[CrossRef](#)]
40. Maley, J.H.; Lasker, G.F.; Kadowitz, P.J. Nitric oxide and disorders of the erythrocyte: Emerging roles and therapeutic targets. *Cardiovasc. Haematol. Disord. Drug Targets* **2010**, *10*, 284–291. [[CrossRef](#)]
41. Gladwin, M.T.; Kato, G.J.; Weiner, D.; Onyekwere, O.C.; Dampier, C.; Hsu, L.; Hagar, R.W.; Howard, T.; Nuss, R.; Okam, M.M. Nitric oxide for inhalation in the acute treatment of sickle cell pain crisis: A randomized controlled trial. *JAMA* **2011**, *305*, 893–902. [[CrossRef](#)]
42. Martinez-Ruiz, R.; Montero-Huerta, P.; Hromi, J.; Head, C.A. Inhaled nitric oxide improves survival rates during hypoxia in a sickle cell (SAD) mouse model. *J. Am. Soc. Anesthesiol.* **2001**, *94*, 1113–1118. [[CrossRef](#)]
43. Cabrales, P.; Han, G.; Nacharaju, P.; Friedman, A.J.; Friedman, J.M. Reversal of hemoglobin-induced vasoconstriction with sustained release of nitric oxide. *Am. J. Physiol.-Heart Circ. Physiol.* **2011**, *300*, H49–H56. [[CrossRef](#)]
44. Kaur, J.; Bhardwaj, A.; Huang, Z.; Narang, D.; Chen, T.-Y.; Plane, F.; Knaus, E.E. Synthesis and biological investigations of nitric oxide releasing nateglinide and meglitinide type II antidiabetic prodrugs: In-vivo antihyperglycemic activities and blood pressure lowering studies. *J. Med. Chem.* **2012**, *55*, 7883–7891. [[CrossRef](#)]
45. Nacharaju, P.; Friedman, A.J.; Friedman, J.M.; Cabrales, P. Exogenous nitric oxide prevents cardiovascular collapse during hemorrhagic shock. *Resuscitation* **2011**, *82*, 607–613. [[CrossRef](#)]

46. Velázquez, C.; Praveen Rao, P.; Knaus, E.E. Novel nonsteroidal antiinflammatory drugs possessing a nitric oxide donor diazen-1-ium-1, 2-diolate moiety: Design, synthesis, biological evaluation, and nitric oxide release studies. *J. Med. Chem.* **2005**, *48*, 4061–4067. [[CrossRef](#)]
47. Napoli, C.; Ignarro, L.J. Nitric oxide-releasing drugs. *Annu. Rev. Pharmacol. Toxicol.* **2003**, *43*, 97–123. [[CrossRef](#)]
48. Andrade, C.; Barros, L.; Lima, M.; Azero, E. Purification and characterization of human hemoglobin: Effect of the hemolysis conditions. *Int. J. Biol. Macromol.* **2004**, *34*, 233–240. [[CrossRef](#)]
49. Safo, M.K.; Abraham, D.J. X-ray crystallography of hemoglobins. In *Hemoglobin Disorders*; Humana Press Inc: Totowa, NJ, USA, 2003; p. 1.
50. Gavrilá, A.; Andersen, L.; Skrydstrup, T. A convenient and simple procedure for the preparation of nitrate esters from alcohols employing $\text{LiNO}_3/(\text{CF}_3\text{CO})_2\text{O}$. *Tetrahedron Lett.* **2005**, *46*, 6205–6207. [[CrossRef](#)]
51. Xu, G.G.; Deshpande, T.M.; Ghatge, M.S.; Mehta, A.Y.; Omar, A.S.M.; Ahmed, M.H.; Venitz, J.; Abdulmalik, O.; Zhang, Y.; Safo, M.K. Design, Synthesis, and Investigation of Novel Nitric Oxide (NO)-Releasing Prodrugs as Drug Candidates for the Treatment of Ischemic Disorders: Insights into NO-Releasing Prodrug Biotransformation and Hemoglobin–NO Biochemistry. *Biochemistry* **2015**, *54*, 7178–7192. [[CrossRef](#)]
52. Winn, M.D.; Ballard, C.C.; Cowtan, K.D.; Dodson, E.J.; Emsley, P.; Evans, P.R.; Keegan, R.M.; Krissinel, E.B.; Leslie, A.G.; McCoy, A. Overview of the CCP4 suite and current developments. *Acta Crystallogr. D Biol. Crystallogr.* **2011**, *67*, 235–242. [[CrossRef](#)]
53. Adams, P.D.; Afonine, P.V.; Bunkóczi, G.; Chen, V.B.; Echols, N.; Headd, J.J.; Hung, L.-W.; Jain, S.; Kapral, G.J.; Kunstleve, R.W.G. The Phenix software for automated determination of macromolecular structures. *Methods* **2011**, *55*, 94–106. [[CrossRef](#)] [[PubMed](#)]
54. Echols, N.; Grosse-Kunstleve, R.W.; Afonine, P.V.; Bunkóczi, G.; Chen, V.B.; Headd, J.J.; McCoy, A.J.; Moriarty, N.W.; Read, R.J.; Richardson, D.C. Graphical tools for macromolecular crystallography in PHENIX. *J. Appl. Crystallogr.* **2012**, *45*, 581–586. [[CrossRef](#)] [[PubMed](#)]
55. Brünger, A.T.; Adams, P.D.; Clore, G.M.; DeLano, W.L.; Gros, P.; Grosse-Kunstleve, R.W.; Jiang, J.-S.; Kuszewski, J.; Nilges, M.; Pannu, N.S. Crystallography & NMR system: A new software suite for macromolecular structure determination. *Acta Crystallogr. D Biol. Crystallogr.* **1998**, *54*, 905–921. [[PubMed](#)]
56. Thatcher, G.R.; Nicolescu, A.C.; Bennett, B.M.; Toader, V. Nitrates and NO release: Contemporary aspects in biological and medicinal chemistry. *Free Radic. Biol. Med.* **2004**, *37*, 1122–1143. [[CrossRef](#)]
57. Wang, E.Q.; Balthasar, J.P.; Fung, H.-L. Pharmacodynamics of in vivo nitroglycerin tolerance in normal conscious rats: Effects of dose and dosing protocol. *Pharm. Res.* **2004**, *21*, 114–120. [[CrossRef](#)]
58. Ahmed, M.H.; Ghatge, M.S.; Safo, M.K. Hemoglobin: Structure, function and allostery. In *Vertebrate and Invertebrate Respiratory Proteins, Lipoproteins and Other Body Fluid Proteins*; Springer Nature: Cham, Switzerland, 2020; pp. 345–382.
59. Silva, M.M.; Rogers, P.H.; Arnone, A. A third quaternary structure of human hemoglobin A at 1.7-Å resolution. *J. Biol. Chem.* **1992**, *267*, 17248–17256. [[CrossRef](#)]
60. Fermi, G.; Perutz, M.F.; Shaanan, B.; Fourme, R. The crystal structure of human deoxyhaemoglobin at 1.74 Å resolution. *J. Mol. Biol.* **1984**, *175*, 159–174. [[CrossRef](#)]
61. Abraham, D.J.; Safo, M.K.; Boyiri, T.; Danso-Danquah, R.E.; Kister, J.; Poyart, C. How allosteric effectors can bind to the same protein residue and produce opposite shifts in the allosteric equilibrium. *Biochemistry* **1995**, *34*, 15006–15020. [[CrossRef](#)]